International Journal of Psychosocial Rehabilitation, Vol. 23, Issue 03, 2019
ISSN: 1475-7192

Design Estimation of the Amount of Solar Radiation Entering Automobile Glazing

N. Lenin Rakesh, G. Anbazhagan and Suriyakumar Jayabal

Abstract--- *The amount of solar radiation entering a closed volume, say a building or an automobile is one of the major challenges to achieve creature comfort inside that closed volume. Automatic air conditioning systems are more common nowadays where sensors are being used to determine the incident solar radiation inside the comfort zone. An attempt is made in this research to replace such costly sensors and complex control logic with a simple algorithm to estimate the amount of solar radiation based on time and geographical data. This calculation of clear-sky solar radiation on any receiving surface on earth whether an automobile surface under motion or a static fenestration of a building is derived based on historical data of select geographical locations in the world.*

Keywords--- *Automobile, Calculation, Clear-sky, Fenestration, Glazing, Heat Load Estimation, Solar Angle, Solar Radiation, Windshield Glass.*

I. INTRODUCTION

Automobiles are equipped with transparent or translucent surfaces in order to enable the driver/passenger, view outside the automobile. Heat energy from sun will pass through such surfaces and enter into the passenger cabin. This heat has to be removed continuously from the cabin to maintain the comfort conditions of the driver/passenger. Hence the knowledge of amount of solar heat radiation entering the passenger cabin is vital for designing any car air-conditioning system. The same principle can be applied to buildings as well since buildings have a number of fenestration/glazing all around them for outside view and natural lighting.

The heat load from solar radiation can be estimated using established equations and known principles, thereby enabling an air-conditioning engineer to include these in his calculation for design purposes. Alternatively the algorithm or logic which is derived could be used in the programming of control logic used in automatic air-conditioning systems.

II. SCOPE OF RESEARCH

This research applies to the calculation of clear-sky solar radiation on any receiving surface on earth whether an automobile surface under motion or a static fenestration of a building. The calculation is only for clear-sky conditions i.e. not for a cloudy or turbid sky. Few of the constants used in the calculation are available only for 5300 known locations in the world (Appendix A). For locations other than these, these constants need to be derived statistically based on record of meteorological data in that particular location and is out of scope of this research.

N. Lenin Rakesh, Assistant Professor, Department of Mechanical Engineering, BIST, BIHER, Bharath Institute of Higher Education & Research, Selaiyur, Chennai.
G. Anbazhagan, Assistant Professor, Department of Mechanical Engineering, BIST, BIHER, Bharath Institute of Higher Education & Research, Selaiyur, Chennai.
Suriyakumar Jayabal, UG Scholar, Department of Mechanical Engineering, BIST, BIHER, Bharath Institute of Higher Education & Research, Selaiyur, Chennai.

Received: 20 Feb 2019 | Revised: 09 Mar 2019 | Accepted: 02 Apr 2019

Calculation for a curved surface is not covered and hence this calculation requires the receiving surface to be flat in a single plane. Surfaces of greater radius of curvature (with arc length to arc depth ratio of greater than 20) can be assumed to be flat and this procedure can be applied.

This calculation is generic and cannot be construed as the worst possible solar radiation that could occur in a specific location on an actual day. Anyhow, this methodology is proven and can be used for design purposes with enough design factor of safety to accommodate real-world worst case situations. A sophisticated broadband radiation model has been derived from the base of REST2 high performance two band clear-sky radiation model [1]. The calculation is based on following assumptions. Any deviation from these assumptions should include a proper safety factor for design purposes.

1) *The sky is clear and free from cloud or turbidity.*
2) *Earth's atmosphere is assumed to be of uniform thickness all around the earth.*
3) All effects of gravity on light are neglected.
4) *All angles mentioned are in degrees.*
5) *The number of days in a year is 365 and leap years are not considered or have to be approximated accordingly*.
6) *The receiving surfaces are flat or of negligible curvature.*
7) *The north-south axis refers to the line connecting the geographical north and south poles and has no reference earth's magnetic north-south axis.*
8) *The shape of the earth is considered to be spherical and not geoid. Hence the determination of angles is purely based on spherical geometry.*
9) *Altitude effects are not considered and it is assumed that angles are calculated at sea levels. However the equations involving the determination of solar radiation have factors which depend on location-specific parameters such as elevation, precipitable water content, aerosols etc.*
10) *All azimuths in this standard are referring geographical south of the earth as the reference direction while some software and books are found to refer geographical north as the reference for angular displacement related to azimuths.*
11) *The day of the equinoxes mentioned in this standard might differ by a day ahead or behind the actual equinox days.*
12) *The pseudo optical depth values used in the calculation are accurate only up to solar zenith angle of 75° beyond which the solar radiation also is not significant to cause worst case situations.*
13) *All pictures or illustrations refer to the day 51, February 20 of the year at New Delhi, India*

III. TERMINOLOGY

Standard terminology is used as per industry practices.

Heating, Ventilation and Air Conditioning (HVAC)

The unit which maintains the human comfort by regulating the temperature and humidity of a closed space by means of heating, cooling and dehumidifying the supply air.

This unit also ventilates the zone which enables normal respiration of occupants.

Irradiance

Irradiance is the power per unit area of electromagnetic radiation incident on a surface.

Fenestration

Fenestration is an arrangement of glass windows, skylight and door systems in a building (usually) or an automobile which serves as visual connection to the outdoors.

Latitude of site

Latitudes are parallels (imaginary lines) which run east to west along the earth's surface.

Longitude of site

Longitudes are meridians (imaginary lines) which run north and south along the surface of the earth.

Apparent solar time (AST)

Apparent solar time is the time derived from the actual, observed motion of the sun. An apparent solar day is the interval between successive returns of the sun to the local meridian.

Mean solar time

Mean solar time is the time derived from a constant day of a fictitious motion of sun. A mean solar day is derived mathematically based on long term observations and consists of exactly 24 hours of a constant running clock.

Equation of time (ET)

The difference between the apparent solar time and the mean solar time is known as/given by the equation of time.

Local standard time (LST)

The time which is followed at the local meridian for day-to-day activities is known as local standard time.

Coordinated universal time (UTC)

Coordinated universal time is the time standard which closely follows the universal time (mean solar time at Royal Observatory, Greenwich – Prime Meridian) and is used for expressing different time zones across the world either as positive or negative offsets.

Time zone (TZ)

Time zone is a region on Earth that has a uniform, legally mandated standard time usually referred to as the local standard time.

Received: 20 Feb 2019 | Revised: 09 Mar 2019 | Accepted: 02 Apr 2019

Daylight saving time (DST)

Daylight saving time is the time followed in certain regions which is usually 1 hour ahead (usually) or behind the local standard time to utilize the available daylight in the region to a maximum.

Solar constant E_{sc}

The solar constant E_{sc} is defined as the intensity of solar radiation on a surface normal to the sun's rays, just beyond the earth's atmosphere, at the average earth-sun distance.

Extraterrestrial radiant flux E_0

Extraterrestrial radiant flux is the amount of solar radiation on a surface normal to sun's rays and of unit surface area, just beyond the earth's atmosphere.

Solar declination angle δ

The angle between the earth-sun line and the equatorial plane is called the solar declination angle.

Solar altitude angle β

The angle between the line emanating from the sun (direct rays from sun) and the horizontal plane of the observer is called the solar altitude angle.

Solar azimuth angle ϕ

The angle between the projection of the line emanating from sun on the horizontal plane to the observer's south is called the solar azimuth angle.

Solar zenith angle ζ

The angle between the line emanating from the sun and the normal (vertical) to the observer's horizontal plane is called the zenith angle.

Hour angle H

The angle between the current location meridian and the meridian which has shortest distance to sun is called the Hour angle.

Relative air mass m

The ratio of the mass of atmosphere at current sun-observer path to the mass of atmosphere directly overhead the observer (or as if when the sun is directly overhead) is called the relative air mass.

Beam normal irradiance E_b

The amount of solar radiation emerging from the solar disc and measured along the direction perpendicular to the rays of the sun is known as beam normal irradiance.

Diffuse horizontal irradiance E_d

The amount of solar radiation emerging from the sky dome, other than the solar disc and measured along the horizontal surface is known as diffuse horizontal irradiance.

Diffuse irradiance vertical-horizontal ratio Y

The ratio of clear-sky diffuse irradiance on a vertical surface to clear-sky diffuse irradiance on a horizontal surface is known as diffuse irradiance vertical-horizontal ratio.

Ground-reflected irradiance E_r

The amount of solar radiation originating from the ground in front of the receiving surface and is directed towards the receiving surface is known as ground-reflected irradiance.

Tilt angle or slope Σ

The angle between the receiving surface and the observer's horizontal plane is called the slope or the tilt angle.

Surface azimuth angle ψ

The angle between the projection of the line normal to the receiving surface on the horizontal plane and the observer's south is called the surface azimuth angle.

Surface – solarazimuth angle γ

The angular difference between the solar azimuth and the surface azimuth is called the surface-solar azimuth angle.

Angle of incidence or Incident angle θ

The angle between the line emanating from sun and the line normal to the receiving surface is known as the angle of incidence or the incident angle.

Clear-sky pseudo optical depths τ

Clear-sky pseudo optical depths are location-specific parameters which embody the dependence of solar radiation upon local conditions like elevation etc. These are pseudo constants since optical depths are used only when relative air mass is unity and is used in this research for convenience only.

Transmissivity Υ

Transmissivity is the fraction of incident radiation which passes through the object (receiving surface). It is also called the coefficient of transmittance.

IV. Determination Of Angles

Solar radiation reaching the earth's surface when the sky is clear (cloudless) is known as clear-sky solar radiation. Usually, a clear-sky day is considered to have the peak solar heat gain compared to a cloudy or turbid day. However, at few locations it has been observed that the peak solar heat gain had been recorded on a cloudy day and was higher than those of the clear-sky radiation values calculated by this. These occurrences are statistically proven to have fewer occurrences and hence neglected for general HVAC design calculations. Solar radiation on a cloudy day can be calculated by introducing a dimensionless factor called clearness number and is out of scope of this research.

Received: 20 Feb 2019 | Revised: 09 Mar 2019 | Accepted: 02 Apr 2019

International Journal of Psychosocial Rehabilitation, Vol. 23, Issue 03, 2019
ISSN: 1475-7192

There are numerous angles which will be used in the calculation and hence a thorough understanding of them is necessary to proceed with the calculation section.

Solar Declination Angle

Earth's orbit is an eclipse (almost circular) with a minor eccentricity of about 0.0167. The largest distance to sun occurs at aphelion and the shortest occurs at perihelion. The plane in which the earth revolves around the sun is called orbital plane or the ecliptic. Earth is split into two halves north and south of earth's self-rotation by an imaginary plane called equatorial plane. The equatorial plane is tilted by an angle of 23.45° to the ecliptic. When the earth moves from one point to another, the equatorial plane shifts parallel between the previous and the current location. In other words, the geographical north- south axis of the earth translates along earth's orbit around sun.

The angle between the earth-sun line and the equatorial plane is called the solar declination angle. This angle varies throughout the year and is responsible for causing seasons like summer, fall, winter and spring.

The declination angle can be approximated to

$$\delta = 23.45 \sin\left(360° \frac{n + 284}{365}\right)$$

Where δ is the solar declination angle

n is the day of year (1 for Jan 1, 32 for Feb 1 etc.)

Sunrays are almost parallel to each other (even pole to pole variation is less than 0.6° due to the vast distance from sun to earth); hence the ray which strikes the equator and the ray which strikes the pole are parallel to each other. The equatorial plane is always oriented at some angle to these sunrays. This angle in other words is the declination angle. If the rays are parallel to the equatorial plane, declination angle is zero. The solar declination angle becomes the extreme maximum at June 21 and December 21 and becomes zero at March 21 and September 21. It is considered negative if the angular displacement is above the ecliptic and is considered positive, otherwise.

$$-23.45° \leq \delta \leq +23.45°$$

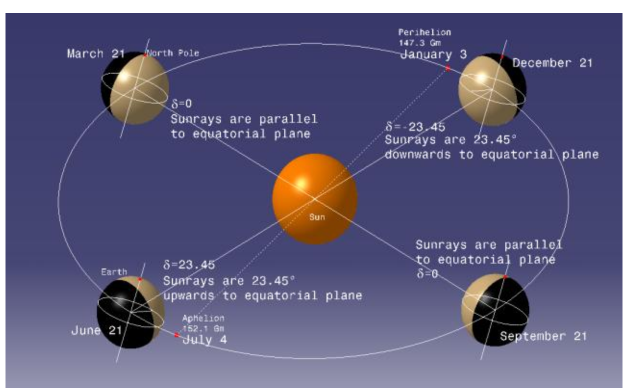

Fig. 1: Solar Declination Angle

Received: 20 Feb 2019 | Revised: 09 Mar 2019 | Accepted: 02 Apr 2019

Solar Altitude Angle

Usually, observer's ground is considered as a horizontal surface and this plane is referred to as the horizontal plane or observer's plane. Note that the orientation of the horizontal plane varies from place to place and is based on observer's location and is always tangential to the earth's surface.

The angle between the line emanating from the sun (direct rays from sun) and the horizontal plane is called the solar altitude angle.

In a typical day, solar altitude angle starts from zero during sunrise reaches the peak value ≤ 90°, by noon and decreases back to zero during the sunset. Negative values correspond to night times. Note in Figure -2 the solar altitude angle at solar noon is little less than 50° and not closer to 90°.

Solar zenith angle is the complement of solar azimuth angle.

$$-90° \leq \beta \leq +90°$$

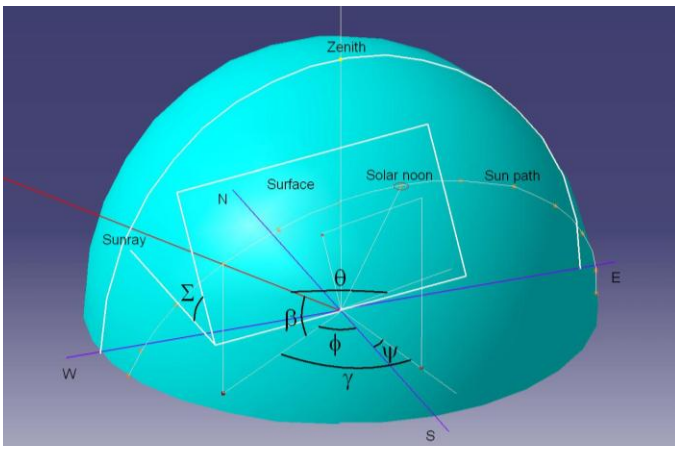

Fig. 2: Solar angles

Solar Azimuth Angle

Earth spins about its own axis and this axis is usually referred to as the north-south axis. This axis is tilted at an angle of 23.45° to the ecliptic vertical (line from earth, perpendicular to ecliptic). Hence for an observer standing on a horizontal plane the direction perpendicularly left to the north-south axis along the horizontal plane is east direction and the direction perpendicularly right to the north-south axis is the west direction. At any instance, the projection of the sun's rays on the horizontal plane gives a reference with respect to the observer's north-south. This angle, the angle between the projection of the sun-observer line on the horizontal plane to the observer's south is called the solar azimuth angle.

Conveniently, the location of the sun in space can be referred with combination of solar altitude angle and solar azimuth angle.

The solar azimuth angle is considered negative for easterly sun's location (morning hours) and is considered positive for westerly sun's location (evening hours). It is zero or 180° at solar noon of everyday. The exact -90° and

International Journal of Psychosocial Rehabilitation, Vol. 23, Issue 03, 2019
ISSN: 1475-7192

+90° occurs at the sunrise and sunset on the day of equinoxes respectively, when the day and night are of equal length.

$$-180° \leq \phi \leq +180°$$

V. Latitude Angle

The imaginary line along the surface of the earth which passes through the equatorial plane is called the equator (Reference x). Similar to equator, concentric circles reducing gradually in diameter can be imagined to stack and form the earth's surface above and below equator. These circles are called latitudes or parallels. The line which emanates from the center of the earth to the latitude forms an angle with the equatorial plane (Refer Figure-3) and this angle is used for the nomenclature of these latitudes, say 10° Latitude, 23° Latitude etc. The latitude at 90° both sides are of diameter zero and are called the north and south poles. Since the latitudes are present on either side of the equator °N or °S are used to denote them uniquely, say 10°N Latitude or 23°S Latitude. The latitude angle in the northern hemisphere is considered positive and in the southern hemisphere it is considered negative.

$$-90° \leq L \leq +90°$$

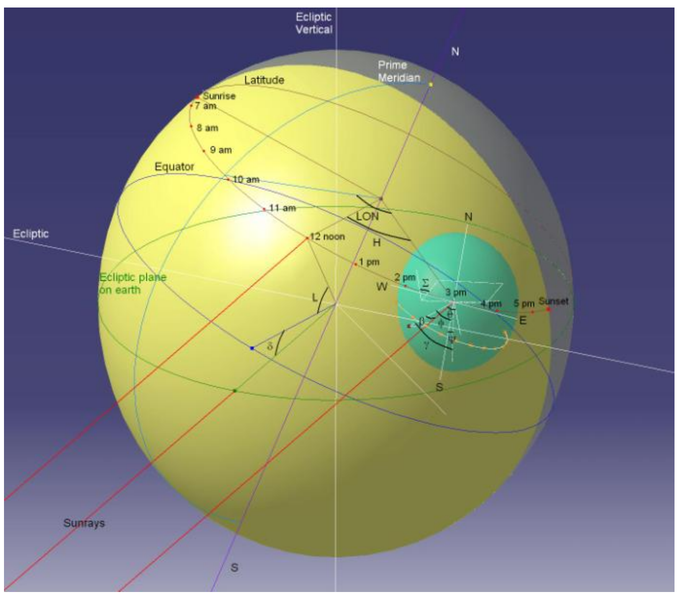

Fig. 3: Earth and Solar angles

VI. Longitude Angle

Longitudes or meridians are imaginary lines which run north and south along the earth's surface, like the linings on a peeled orange (Reference x). The Prime Meridian which passes through Greenwich is considered as the reference meridian from which all other meridians are named. The angle formed by the center of the earth along the equatorial plane from the Prime Meridian is the name of the meridian under consideration; say 15° Longitude or 127° Longitude. The longitudes on left half of the Prime Meridian are °E Longitudes and that on the right side are °W Longitudes. As a sign convention, the latitude angles °E are considered positive and °W are considered negative.

$$-180^\circ \leq LON \leq +180^\circ$$

VII. Hour Angle

Earth's orbit is an ec necessary to proceed with the calculation Solar noon occurs every day when the sun reaches the maximum altitude in the sky (solar altitude angle is maximum). This may not happen exactly by 12 noon of local standard time. The observer (with his local meridian) will be at the shortest observer-sun distance when the solar noon occurs. Hence at any point of time other than solar noon, the observer will be away from this point of shortest distance by a specified angle as per the rotation of the earth.

The angle between the current location meridian and the meridian which has shortest distance to sun is called the Hour Angle. It could be on the east or west side of the observer and is considered negative in the morning hours, positive in the afternoon hours and zero at solar noon. The hour angle will be maximum during sunrise and sunset. In summer the hour angle will be more than 90° and during winter the hour angle will be lesser than 90° on both sides of the observer north-south axis. The latitude which has complete daylight for whole 24 hours but a few seconds of night will tend to have almost -180° and 180° hour angles during sunrise and sunset respectively.

$$-180 \leq H \leq +180^\circ$$

VIII. Tilt Angle or Slope

Vehicle exterior surfaces and in particular fenestration (glass surfaces) will be mostly inclined at arbitrary orientations. The surfaces are fixed to the vehicle body and are passive (not moving with respect to vehicle). These surfaces are referred to as receiving surfaces in this standard. The angle between the receiving surface and the observer's horizontal plane is called the slope of the receiving surface or the tilt angle.

Tilt angle can range from zero to 180°. Zero corresponds to horizontal surfaces (such as roof), 90° corresponds to vertical surfaces (such as window glass), angle greater than 90° corresponds to surfaces facing the ground (such as rear bottom glass in tractors) and 180° corresponds to surfaces which fully face the ground (such as floor).

$$0^\circ \leq \Sigma \leq +180^\circ$$

Surface azimuth angle

A receiving surface can be better specified by its tilt angle along with its orientation along north-south direction. The angle between the projection of the line normal to the receiving surface on the horizontal plane and the observer's south is called the surface azimuth angle. If this lies on the east side of the observer, it is considered negative and on the west side it is considered positive.

$$-180^\circ \leq \psi \leq +180^\circ$$

Surface-solar azimuth angle

The angular difference between the solar azimuth and the surface azimuth is called the surface-solar azimuth angle. The solar azimuth is fixed on a given day, but the surface azimuth can lie anywhere in the horizontal plane since the surface under consideration is an automobile surface and is free to move in any direction as the automobile moves. Due to this the entire 360° has to be covered by the surface-solar azimuth angle in the calculation section with a looping construct. The following simple expression can be used in design calculations keeping the same sign conventions used for solar azimuth and surface azimuth angles.

$$\gamma = \phi - \psi$$

In this case, the solar-surface azimuth angle ranges from -270° to +270° numerically (can be expressed in range of -180° to +180°, if directional sense is captured with some other expression) and can be used directly in calculations without any sign convention. For example, +256 and -104 are same angular orientations since sin(180+x)=sin(180-x) and cos(180+x)=cos(180-x).

The surface-solar azimuth angle can be used to understand whether the surface is in the shade. For tilt angles greater than solar altitude angle, a surface-solar azimuth angle value greater than 90° or lesser than -90° indicates that the surface is in shade. Such surfaces can be excluded from calculations. For tilt angles lesser than solar altitude angle, the sunrays will hit the surface at all azimuth orientations. Caution is required for surfaces which could be partially irradiated which has to be dealt as two or more surfaces as per the area of shading.

$$-270° \leq \gamma \leq +270°$$

Angle of incidence

The angle at which the direct rays from sun strike the receiving surface is very important in estimating solar load.

This angle, the angle between the line emanating from sun and the line normal to the receiving surface is known as the angle of incidence or the incident angle. Every surface has its ability to absorb, transmit or reflect sun's rays and this angle of incidence affects the intensity of direct beam solar radiation striking the surface.

When the sun's rays are directly overhead, the angle of incidence for a horizontal surface is zero and when the rays are almost parallel to the horizontal surface say at sunrise/sunset, the angle of incidence will be its peak (little less than 90°). There is no sign convention for angle of incidence; it is always positive.

$$0° \leq \theta < +90°$$

Relative Air Mass

Assuming earth's atmosphere of uniform radial thickness all around the earth, any radial direction would be the shortest path from extraterrestrial space to the earth's surface. When the sun is directly overhead, sun's rays travel the shortest distance in the atmosphere to reach the observer i.e. when the altitude angle is 90°. When the sun is at any other angle i.e. when the altitude angle is other than 90°, the sun's rays has to travel more distance to reach the observer.

In other words, the mass of atmosphere directly overhead is lesser than the mass of atmosphere at any other angle. The ratio of the mass of atmosphere at current sun-observer path to the mass of atmosphere directly overhead the observer (or as if when the sun is directly overhead) is called the relative air mass.

Since this relative air mass is dependent only on the angular orientation of sun, it can be expressed only in terms of β and can be given as

$$m = \frac{1}{[\sin\beta + 0.50572(6.07995 + \beta)^{-1.6364}]}$$

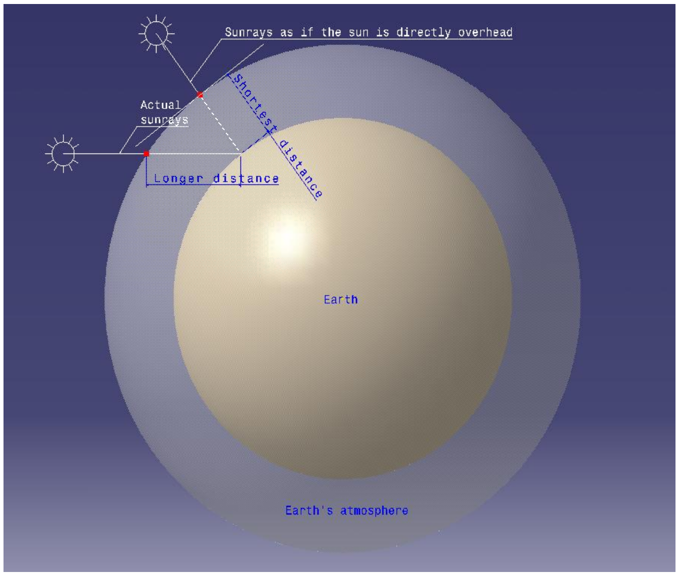

Fig. 4: Relative Air Mass

Motion of the sun around the observer

Earth is revolving around the sun and spins in its own axis. The sun is almost stationary on a given day while the earth spins from east to west. For an observer, who is at a specific coordinate on earth's surface, the sun will seem to move from one direction to other in a specific path. This path can be traced on an imaginary bowl around the observer to understand this phenomenon. As well as this could give clear idea about various angles involved in this calculation section.

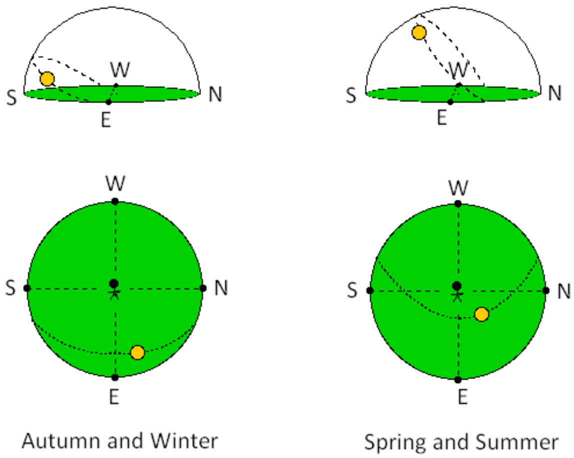

Fig. 5: Seasons

Received: 20 Feb 2019 | Revised: 09 Mar 2019 | Accepted: 02 Apr 2019

The sun does not travel perfect east to west every day. In northern hemisphere, during the seasons of spring and summer, the sun rises in the northeast and follow a long, high arc and sets in the northwest direction. The days will be longer than nights. During autumn and winter, the sun rises in the southeast and follows a low, short arc and sets in the southwest direction.

The same situations will be reverse in the southern hemisphere. Only on vernal and autumnal equinoxes (Mar 21 and Sep 21) the sun will rise in the exact east direction and set in the exact west direction thus making the solar azimuth angle exact 90° during sunrise and sunset. In other days, the azimuth angle of 90° could possibly happen only when the sun is up in the sky (β>0°) and traverses from north to south or vice versa intersecting the east-west plane.

The altitude angle is 90° only when the sun is exactly overhead. This would happen twice in a year for the latitudes which lie between the Tropic of Cancer and the Tropic of Capricorn and only once in the exact tropics during solstices. For all latitudes outside this range, the solar altitude never reaches 90°.

Spring and summer will have sunlight more than 12 hours a day and fall and winter will have daylight less than 12 hours.

Due to this, the hour angle range may exceed 90° in spring and summer on both sides of the solar noon with alternate signs. The hour angle range will be lesser than 90° on both sides in fall and winter.

IX. Calculation

Extraterrestrial solar radiation

Various gases within the earth’s atmosphere absorb some solar radiation at different wavelengths, and clouds and dust also affect it. Hence the solar radiation flux that reaches the earth’s surface will be lesser than that just beyond the earth’s atmosphere. The extraterrestrial radiant flux normal to the sun’s rays will be varying throughout the year since the earth follows an approximate elliptical orbit (almost a circular orbit) around sun and the earth-sun distance varies throughout the year. This variation reaches a maximum of 1412 W/m2 and a minimum of 1322 W/m2 when the earth is closest and farthest to the sun respectively. An average value of 1366 W/m2 is observed over the entire orbital motion of the earth. The term solar constant refers to the intensity of solar radiation on a surface normal to sun’s rays, just beyond the earth’s atmosphere, at the average earth-sun distance and is proposed to be 1367 W/m2 by the World Meteorological Organization in 1981.

$$E_{sc} = 1367 \ \frac{W}{m^2}$$

The extraterrestrial solar radiation on any day of the year can be approximated with the following equation.

$$E_0 = E_{sc}\left[1 + 0.033 \cos\left[360^\circ \frac{(n-3)}{365}\right]\right]$$

Where n is the day of year (1 for Jan 1, 32 for Feb 1, 60 for Mar 1 etc.)

Solar time and local time

A solar sundial refers the sun's motion in the sky to displays time and this time will vary with the time shown by a clock running at a uniform rate. This difference is due to the fact that earth's orbital velocity is not constant throughout the year and varies as per its eccentricity and distance towards sun. This variation will be in minutes and not in hours.

The time shown by a sundial is the solar time, otherwise called as the apparent solar time. The time shown by the clock running at a constant rate is usually a reference for the local standard time at a particular location. The difference between these two is expressed in minutes and is given by an equation called equation of time and is approximated

$$ET = 2.2918\,[0.0075 + 0.1868\cos(\Gamma) - 3.2077\sin(\Gamma) - 1.4615\cos(2\Gamma) - 4.089\sin(2\Gamma)]$$

$$-14.1\ min \leq ET \leq +16.55\ min$$

$$where\ \Gamma = 360°\frac{(n-1)}{365}$$

Note that the time at every longitude varies and an approximate local standard time is usually followed in a collective region (time zone) as a whole. This correction needs to be incorporated along with equation of time to get the apparent solar time of that region. This longitude correction is four minutes of time per degree difference between the local standard time followed in that zone and the actual local standard meridian's time.

$$AST = LST + \frac{ET}{60} + (LON - LSM)\frac{4}{60}$$

Where AST is the Apparent Solar Time

LST is the Local Standard Time

LSM is the Local Standard Meridian

The Prime Meridian provides the reference for the all time zones across the world and the time followed along the Prime Meridian is the universal time. Every other zonal time is either added or subtracted to UTC and usually time zones are present every 15° longitude E or W. The entire 360° earth can be split into 24 hours thereby yielding 15° each hour time difference.

These meridians which are hourly credits of UTC are Local Standard Meridians.

$$LSM = 15\ TZ$$

Caution is required since some countries or regions use half-hour or quarter-hour credits from UTC. For example India follows UTC+05:30, Nepal follows UTC+05:45 and the Province of Newfoundland in Canada follows UTC-03:30 as their Local Standard Meridians.

Certain regions in the world follow Daylight Savings Time which is usually one hour ahead (sometimes, one hour behind) of the local standard time of that region. This one hour has to be subtracted to obtain the local standard time of that region to use in calculations.

Received: 20 Feb 2019 | Revised: 09 Mar 2019 | Accepted: 02 Apr 2019

$$LST = DST - 1$$

For example, CDT (Central Daylight-savings Time) is hour ahead of the usual Central Standard Time.

$$CST = CDT - 1$$

Calculation of Amount of Solar Radiation

One hour east or west of solar noon corresponds to 15 degrees of angular displacement along the latitude. The hour angle can be related to apparent solar time as

$$H = 15\ (AST - 12)$$

where AST is in hours (current solar time) and 12 refers to the solar noon.

To start with, the following parameters should be known

- Day of year

- Location (Latitude and Longitude)

- Local Standard Time (time under consideration for calculation)

From these inputs, the following will be derived.

- Day of year - n

- Latitude angle - L

- Longitude angle – LON

- Solar Declination angle - δ

- Equation of Time – ET (Refer Equation x)

- Apparent Solar Time – AST (Refer Equation x)

- Hour Angle – H (Refer Equation x)

- Extraterrestrial Solar Flux – E0 (Refer Equation x)

At any particular instant of daylight, the solar altitude angle and the solar azimuth angle can be given by

$$\beta = \sin^{-1}(\cos L \cos \delta \cos H + \sin L \sin \delta)$$

$$\phi = \sin^{-1}\left(\frac{\sin H \cos \delta}{\cos \beta}\right) = \cos^{-1}\left(\frac{\cos H \cos \delta \sin L - \sin \delta \cos L}{\cos \beta}\right)$$

The relative air mass is only dependent on the solar altitude angle and can be calculated with the following equation

$$m = \frac{1}{[\sin \beta + 0.50572(6.07995 + \beta)^{-1.6364}]}$$

The clear-sky solar radiation is defined by its beam and diffuse components. Usually beam direct radiation (emanating from solar disc) is measured perpendicular to sun's rays and diffuse radiation (emanating from the sky dome except solar disc) is measured along the observer's horizontal plane. These two components of clear-sky solar radiation are given by the following modified Bouguer-Lambert-Beer relations

$$E_b = E_0 e^{-\tau_b m^{ab}}$$

$$E_d = E_0 e^{-\tau_d m^{ad}}$$

where Eb is the beam normal irradiance

Ed is the diffuse horizontal irradiance

m is the relative air mass

τb and τd are the beam and diffuse pseudo-optical lengths

ab and ad are the beam and diffuse air mass exponents and are given by

$$ab = 1.219 - 0.043\tau_b - 0.151\tau_d - 0.204\tau_b\tau_d$$

$$ad = 0.202 - 0.852\tau_b - 0.007\tau_d - 0.357\tau_b\tau_d$$

The unknown parameters in these equations are τb and τd. ASHRAE research project RP-1453 (Reference x) analyzed numerous location-specific solar radiation values and thus derived τb and τd which could be used to calculate the clear-sky beam and diffuse components. The tabulation (Appendix x) is given only for 21st day of every month. Values for other days should be interpolated. Using the τb and τd the beam and diffuse components of clear-sky solar radiation are calculated.

Slope of the vehicle surface is known from vehicle model. The direction in which this surface will face cannot be fixed to a single direction and hence has to be iterated from 0° to 360° to find the worst case direction with maximum solar radiation. Now fixing the slope and azimuth of the receiving surface, we are able to calculate the surface-solar azimuth angle.

Slope - Σ

Surface azimuth angle - ψ

$$\gamma = \phi - \psi$$

The angle of incidence is given by

$$\theta = \cos^{-1}(\cos\beta \cos\gamma \sin\Sigma + \sin\beta \cos\Sigma)$$

The clear-sky solar radiation reaching the receiving surface is of three components, the beam, the diffuse and the ground-reflected component. The beam component is the solar radiation which emanates from the solar disc. The diffuse component is the solar radiation originating from the sky dome (cosmic) other than the solar disc. The ground-reflected component is the solar radiation which is emitted (reflected) from the ground in front of the receiving surface.

$$E_t = E_{t,b} + E_{t,d} + E_{t,r}$$

Beam component is directly affected by the angle of incidence and is given by

$$E_{t,b} = E_b \cos\theta$$

The diffuse component is more difficult to estimate and a simple equation could be used as an approximation which would cater to the needs of basic HVAC design. The diffuse irradiance on the horizontal surface is a simple function of angle of incidence and is given by

$$E_{t,d} = E_d Y$$

where Ed is the diffuse horizontal irradiance (Refer Eqn x)

Y is the diffuse irradiance vertical-horizontal ratio

$$Y = 0.55 + 0.437\cos\theta + 0.313\cos^2\theta$$

The diffuse irradiance on the receiving surface (which is at slope Σ) is given by

$$E_{t,d} = \begin{cases} E_d Y \sin\Sigma + E_d \cos\Sigma & if\ \Sigma \leq 90° \\ E_d Y \sin\Sigma & if\ \Sigma > 90° \end{cases}$$

The ground-reflected component for all orientations is given by

$$E_{t,r} = \rho_g (E_b \sin\beta + E_d)\left(\frac{1-\cos\Sigma}{2}\right)$$

where ρ_g is ground reflectance and is usually taken as 0.2 for a typical mixture of ground surfaces. For surfaces like desert sand and snow 0.4 could be used.

$$\rho_g = 0.2$$

Now all three components are added to obtain the total solar radiation striking the receiving surface.

$$E_t = E_{t,b} + E_{t,d} + E_{t,r}$$

Each and every surface will have some transmissivity properties and only a fraction of the incident radiation will pass through the surface and reaches the cabin space of vehicle which needs to be air-conditioned. This ratio of incident radiation to passed radiation is known as coefficient of transmittance or transmissivityϒ. The amount of radiation which reaches the cabin is given by

$$E = \Upsilon E_t$$

Case Study

For the purpose of case study, a commercial sports utility vehicle (SUV) is considered. The vehicle is subjected to day to day variations of the solar radiation and hence it is prudent to find the frequency of occurrence of maximum solar radiation in a year, say 0.4% of times in a year. This particular solar radiation value can be used in design calculations.

The location under consideration for case study is New Delhi, India (28.57°N Latitude, 77.12°E Longitude, UTC+05:30 IST).

$$L = 28.57°$$

$$LON = 77.12°$$

Table I: Properties of receiving surfaces

Receiving Surface	Tilt Angle Σ	Surface Area A (m^2)
Windshield Glass	44.78°	0.782
Right Side Glass	82.01°	0.587
Back Door Glass	75.58°	0.466
Left Side Glass	82.01°	0.587

The coefficient of transmittance ϒ for all glasses is 0.81 and the side glasses are oriented parallel to the vehicle centre line.

$$TZ = 5.5$$

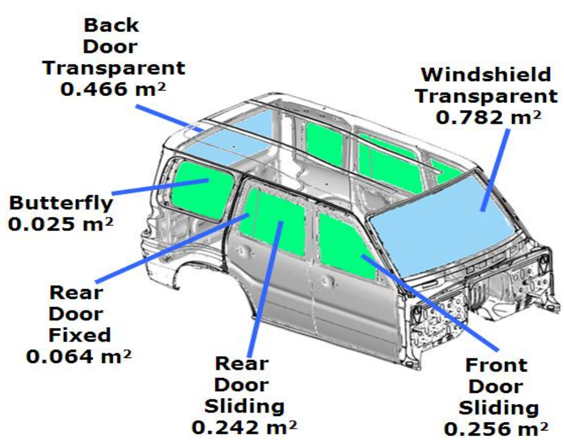

Fig. 6: Surface area of receiving surfaces on vehicle

Since the side glasses (front door, rear door sliding, rear door fixed and butterfly) are oriented at same tilt angles, the following four surfaces can be considered for calculation. Note that even though Side Glass LH and Side Glass RH have same tilt angles they face different directions and cannot be added together.

In a single day of 24 hours, daylight is available only for few hours. For New Delhi it ranges from 10.17 hours to 13.82 hours over the entire year. Hence it is unnecessary to check solar radiation values for the night times. Even sunrise and sunset hours can be excluded from calculations since the air mass ratio will be very high and the solar radiation is not significant. The hours which need to be considered for calculation can be determined easily by finding the maximum hour angle of the day. Equation x gives,

Received: 20 Feb 2019 | Revised: 09 Mar 2019 | Accepted: 02 Apr 2019

$$\sin\beta = \cos L \cos\delta \cos H + \sin L \sin\delta$$

The hour angle will be maximum during sunrise and sunset. In that case, the solar altitude angle will be zero.

$$\beta = 0°$$

Substituting this in Equation x, we get

$$H_{max} = \cos^{-1}(-\tan L \tan\,\delta)$$

Every 15° hour angle corresponds to one hour of apparent solar time. Hence daylight time in hours is given by

$$D = \frac{2H_{max}}{15}$$

The daylight ranges from (12 – D/2) to (12 + D/2) with 12 noon as the symmetry. Note the time discussed here is apparent solar time and not local standard time. LST will vary with AST by Equation x.

Usually for a single receiving surface, the maximum radiation will hit the surface when the surface solar-azimuth angle is zero. In other words, the maximum incident solar radiation will occur when the surface is directly facing the sun. But Scorpio is having 4 different surfaces at different orientations put together. In this case it is difficult to predict the direction of maximum transmitted solar radiation. When LH side glass is sunlit, the RH side glass might be in shade. To account for all possibilities the vehicle has to be rotated from 0° to 360° and capture the direction with maximum transmitted solar radiation. This heat gain will be recorded against the amount of solar radiation for that particular hour of daylight.

The pseudo-optical depths tabulated in the Appendix x gives the following values for 21st day of every month.

Linear interpolation can be used to obtain the values for other days in the month.

$$\tau_b = \tau_{b,m} + \frac{\tau_{b,m+1} - \tau_{b,m}}{dt_{m+1} - dt_m}$$

$$\tau_d = \tau_{d,m} + \frac{\tau_{d,m+1} - \tau_{d,m}}{dt_{m+1} - dt_m}$$

where m+1 denotes the next 21st day

m denotes the previous 21st day

dt is the date

$dt_{m+1} - dt_m$ denotes the number of days in between

The azimuth of windshield is taken as reference for calculating azimuths of other surfaces simultaneously. If windshield faces south, side glasses face east and west and backdoor glass faces north respectively. For a orientation of 30° from south towards east, the surface azimuth angles of all 4 surfaces will be as shown.

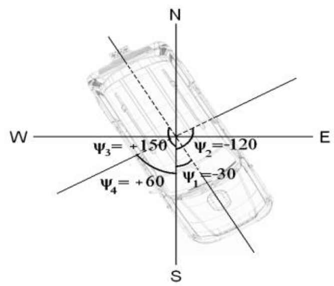

Fig. 7: Azimuth of the vehicle

In general if ψ1 is known, the other three surface azimuth angles can be given by

$$\psi_2 = \begin{cases} \psi_1 - 90° & if -90° \le \psi_1 \le +180° \\ \psi_1 + 270° & otherwise \end{cases}$$

$$\psi_3 = \begin{cases} \psi_1 - 180° & if \quad 0° \le \psi_1 < +180° \\ \psi_1 + 180° & otherwise \end{cases}$$

$$\psi_4 = \begin{cases} \psi_1 + 90° & if -180° \le \psi_1 \le +90° \\ \psi_1 - 270° & otherwise \end{cases}$$

Table II: Pseudo-optical depth values

	Jan	Feb	Mar	Apr	May	Jun
τ_b	0.552	0.572	0.592	0.707	0.937	1.015
τ_d	1.649	1.603	1.589	1.421	1.208	1.181
	Jul	Aug	Sep	Oct	Nov	Dec
τ_b	1.060	0.901	0.703	0.863	0.772	0.569
τ_d	1.169	1.285	1.493	1.255	1.333	1.612

Algorithm

A sample algorithm is attempted to simulate the calculation. The function MOD used in the algorithm denotes the remainder of a division operation.

$L = 28.57$

$E_{sc} = 1367$

$\rho_g = 0.2$

$\Sigma_1 = 44.78$

$\Sigma_2 = 82.01$

$\Sigma_3 = 75.58$

$\Sigma_4 = 82.01$

$A_1 = 0.782$

$\mathrm{A}_2 = 0.587$

$\mathrm{A}_3 = 0.466$

$\mathrm{A}_4 = 0.587$

$\tau_{b,1} = \cdots$

$\tau_{b,2} = \cdots$

$\cdots$

$\tau_{b,8760} = \cdots$

$\tau_{d,1} = \cdots$

$\tau_{b,2} = \cdots$

$\cdots$

$\tau_{d,8760} = \cdots$

$FOR\ h = 1\ to\ 8760$

$$n == \frac{h - MOD(h, 24)}{24}$$

$$\delta = 23.45 \sin\left(360° \frac{n + 284}{365}\right)$$

$$E_0 = E_{sc}\left[1 + 0.033 \cos\left[360° \frac{(n - 3)}{365}\right]\right]$$

$AST = MOD(h, 24)$

$H_{max} = \cos^{-1}(-\tan L \tan \delta)$

$$D = \frac{2H_{max}}{15}$$

$IF\ AST < (12 - D/2)\ OR\ AST > (12 + D/2)\ THEN$

$E_h = 0$

$ELSE$

$H = 15\ (AST - 12)$

$\beta = \sin^{-1}(\cos L \cos \delta \cos H + \sin L \sin \delta)$

$$\phi = \sin^{-1}\left(\frac{\sin H \cos \delta}{\cos \beta}\right)$$

Received: 20 Feb 2019 | Revised: 09 Mar 2019 | Accepted: 02 Apr 2019

International Journal of Psychosocial Rehabilitation, Vol. 23, Issue 03, 2019
ISSN: 1475-7192

$$m = \frac{1}{[\sin\beta + 0.50572(6.07995 + \beta)^{-1.6364}]}$$

$$ab = 1.219 - 0.043\tau_{b,h} - 0.151\tau_{d,h} - 0.204\tau_{b,h}\tau_{d,h}$$

$$ad = 0.202 - 0.852\tau_{b,h} - 0.007\tau_{d,h} - 0.357\tau_{b,h}\tau_{d,h}$$

$$E_b = E_0 e^{-\tau_{b,h} m^{ab}}$$

$$E_d = E_0 e^{-\tau_{d,h} m^{ad}}$$

$$E_{max} = 0$$

$$FOR\ a = -180\ to\ +179$$

$$\psi_1 = a$$

$$\psi_2 = \begin{cases} \psi_1 - 90^\circ & if - 90^\circ \le \psi_1 \le +180^\circ \\ \psi_1 + 270^\circ & otherwise \end{cases}$$

$$\psi_3 = \begin{cases} \psi_1 - 180^\circ & if \quad 0^\circ \le \psi_1 < +180^\circ \\ \psi_1 + 180^\circ & otherwise \end{cases}$$

$$\psi_4 = \begin{cases} \psi_1 + 90^\circ & if - 180^\circ \le \psi_1 \le +90^\circ \\ \psi_1 - 270^\circ & otherwise \end{cases}$$

$$\gamma_1 = \phi - \psi_1$$

$$\gamma_2 = \phi - \psi_2$$

$$\gamma_3 = \phi - \psi_3$$

$$\gamma_4 = \phi - \psi_4$$

$$\theta_1 = \cos^{-1}(\cos\beta\cos\gamma_1\sin\Sigma_1 + \sin\beta\cos\Sigma_1)$$

$$\theta_2 = \cos^{-1}(\cos\beta\cos\gamma_2\sin\Sigma_2 + \sin\beta\cos\Sigma_2)$$

$$\theta_3 = \cos^{-1}(\cos\beta\cos\gamma_3\sin\Sigma_3 + \sin\beta\cos\Sigma_3)$$

$$\theta_4 = \cos^{-1}(\cos\beta\cos\gamma_4\sin\Sigma_4 + \sin\beta\cos\Sigma_4)$$

$$E_{1,t,b} = E_b\cos\theta_1$$

$$E_{2,t,b} = E_b\cos\theta_2$$

$$E_{3,t,b} = E_b\cos\theta_3$$

$$E_{4,t,b} = E_b\cos\theta_4$$

$$Y_1 = 0.55 + 0.437\cos\theta_1 + 0.313\cos^2\theta_1$$

$$Y_2 = 0.55 + 0.437\cos\theta_2 + 0.313\cos^2\theta_2$$

$$Y_3 = 0.55 + 0.437\cos\theta_3 + 0.313\cos^2\theta_3$$

Received: 20 Feb 2019 | Revised: 09 Mar 2019 | Accepted: 02 Apr 2019

$$Y_4 = 0.55 + 0.437 \cos\theta_4 + 0.313 \cos^2\theta_4$$

$$E_{1,t,d} = \begin{cases} E_d Y_1 \sin\Sigma_1 + E_d \cos\Sigma_1 & if\ \Sigma_1 \le 90° \\ E_d Y_1 \sin\Sigma_1 & if\ \Sigma_1 > 90° \end{cases}$$

$$E_{2,t,d} = \begin{cases} E_d Y_2 \sin\Sigma_2 + E_d \cos\Sigma_2 & if\ \Sigma_2 \le 90° \\ E_d Y_2 \sin\Sigma_2 & if\ \Sigma_2 > 90° \end{cases}$$

$$E_{3,t,d} = \begin{cases} E_d Y_3 \sin\Sigma_3 + E_d \cos\Sigma_3 & if\ \Sigma_3 \le 90° \\ E_d Y_3 \sin\Sigma_3 & if\ \Sigma_3 > 90° \end{cases}$$

$$E_{4,t,d} = \begin{cases} E_d Y_4 \sin\Sigma_4 + E_d \cos\Sigma_4 & if\ \Sigma_4 \le 90° \\ E_d Y_1 \sin\Sigma_4 & if\ \Sigma_4 > 90° \end{cases}$$

$$E_{1,t,r} = \rho_g (E_b \sin\beta + E_d)\left(\frac{1-\cos\Sigma_1}{2}\right)$$

$$E_{2,t,r} = \rho_g (E_b \sin\beta + E_d)\left(\frac{1-\cos\Sigma_2}{2}\right)$$

$$E_{3,t,r} = \rho_g (E_b \sin\beta + E_d)\left(\frac{1-\cos\Sigma_3}{2}\right)$$

$$E_{4,t,r} = \rho_g (E_b \sin\beta + E_d)\left(\frac{1-\cos\Sigma_4}{2}\right)$$

$$E_{1,t} = E_{1,t,b} + E_{1,t,d} + E_{1,t,r}$$

$$E_{2,t} = E_{2,t,b} + E_{2,t,d} + E_{2,t,r}$$

$$E_{3,t} = E_{3,t,b} + E_{3,t,d} + E_{3,t,r}$$

$$E_{4,t} = E_{4,t,b} + E_{4,t,d} + E_{4,t,r}$$

$$E = \Upsilon A_1 E_{1,t} + \Upsilon A_2 E_{2,t} + \Upsilon A_3 E_{3,t} + \Upsilon A_4 E_{4,t}$$

$IF\ E > E_{max}\ THEN$

$E_{max} = E$

$ENDIF$

$NEXT$

$E_h = E_{max}$

$ENDIF$

$NEXT$

$OUTPUT\ E_h$

X. CONCLUSION

The output from the algorithm E_h (E_1, $E_2 \ldots E_{8760}$) is an array which will hold the values for amount of solar radiation getting inside the vehicle for every hour of the year. On sorting out the array, it is possible to identify the design value which occurs 0.4% times highest in a year and could be used in HVAC design calculations. Extending this algorithm further work can be carried out to incorporate such calculation directly into the control logic of the vehicle.

REFERENCES

[1] Thooyamani, K.P., Khanaa, V., & Udayakumar, R. (2014). Virtual instrumentation based process of agriculture by automation. *Middle-East Journal of Scientific Research*, *20*(12): 2604-2612.
[2] Udayakumar, R., Kaliyamurthie, K.P., & Khanaa, T.K. (2014). Data mining a boon: Predictive system for university topper women in academia. *World Applied Sciences Journal*, *29*(14): 86-90.
[3] Anbuselvi, S., Rebecca, L.J., Kumar, M.S., & Senthilvelan, T. (2012). GC-MS study of phytochemicals in black gram using two different organic manures. *J Chem Pharm Res*., *4*, 1246-1250.
[4] Subramanian, A.P., Jaganathan, S.K., Manikandan, A., Pandiaraj, K.N., Gomathi, N., & Supriyanto, E. (2016). Recent trends in nano-based drug delivery systems for efficient delivery of phytochemicals in chemotherapy. *RSC Advances*, *6*(54), 48294-48314.
[5] Thooyamani, K.P., Khanaa, V., & Udayakumar, R. (2014). Partial encryption and partial inference control based disclosure in effective cost cloud. *Middle-East Journal of Scientific Research*, 20(12), 2456-2459.
[6] Lingeswaran, K., Prasad Karamcheti, S.S., Gopikrishnan, M., & Ramu, G. (2014). Preparation and characterization of chemical bath deposited cds thin film for solar cell. *Middle-East Journal of Scientific Research*, *20*(7), 812-814.
[7] Maruthamani, D., Vadivel, S., Kumaravel, M., Saravanakumar, B., Paul, B., Dhar, S.S., Manikandan, A., & Ramadoss, G. (2017). Fine cutting edge shaped Bi2O3rods/reduced graphene oxide (RGO) composite for supercapacitor and visible-light photocatalytic applications. *Journal of colloid and interface science*, *498*, 449-459.
[8] Gopalakrishnan, K., Sundeep Aanand, J., & Udayakumar, R. (2014). Electrical properties of doped azopolyester. *Middle-East Journal of Scientific Research*, *20*(11). 1402-1412.
[9] Subhashree, A.R., Parameaswari, P.J., Shanthi, B., Revathy, C., & Parijatham, B.O. (2012). The reference intervals for the haematological parameters in healthy adult population of chennai, southern India. *Journal of Clinical and Diagnostic Research: JCDR*, *6*(10), 1675-1680.
[10] Niranjan, U., Subramanyam, R.B.V., & Khanaa, V. (2010, September). Developing a web recommendation system based on closed sequential patterns. In *International Conference on Advances in Information and Communication Technologies, 101*, 171-179. Springer, Berlin, Heidelberg.
[11] Slimani, Y., Baykal, A., & Manikandan, A. (2018). Effect of Cr3+ substitution on AC susceptibility of Ba hexaferrite nanoparticles. *Journal of Magnetism and Magnetic Materials*, *458*, 204-212.
[12] Premkumar, S., Ramu, G., Gunasekaran, S., & Baskar, D. (2014). Solar industrial process heating associated with thermal energy storage for feed water heating. *Middle East Journal of Scientific Research*, *20*(11), 1686-1688.
[13] Kumar, S.S., Karrunakaran, C.M., Rao, M.R.K., & Balasubramanian, M.P. (2011). Inhibitory effects of Indigofera aspalathoides on 20-methylcholanthrene-induced chemical carcinogenesis in rats. *Journal of carcinogenesis*, *10*.
[14] Beula Devamalar, P.M., Thulasi Bai, V., & Srivatsa, S.K. (2009). Design and architecture of real time web-centric tele health diabetes diagnosis expert system. *International Journal of Medical Engineering and Informatics*, *1*(3), 307-317.
[15] Ravichandran, A.T., Srinivas, J., Karthick, R., Manikandan, A., & Baykal, A. (2018). Facile combustion synthesis, structural, morphological, optical and antibacterial studies of Bi1− xAlxFeO3 (0.0≤ x≤ 0.15) nanoparticles. *Ceramics International*, *44*(11), 13247-13252.
[16] Thovhogi, N., Park, E., Manikandan, E., Maaza, M., & Gurib-Fakim, A. (2016). Physical properties of CdO nanoparticles synthesized by green chemistry via Hibiscus Sabdariffa flower extract. *Journal of Alloys and Compounds*, *655*, 314-320.
[17] Thooyamani, K.P., Khanaa, V., & Udayakumar, R. (2014). Wide area wireless networks-IETF. *Middle-East Journal of Scientific Research*, *20*(12), 2042-2046.
[18] Sundar Raj, M., Saravanan, T., & Srinivasan, V. (2014). Design of silicon-carbide based cascaded multilevel inverter. *Middle-East Journal of Scientific Research*, *20*(12), 1785- 1791.
[19] Achudhan, M., Jayakumar M.P. (2014). Mathematical modeling and control of an electrically-heated catalyst. *International Journal of Applied Engineering Research*, *9*(23), 23013.

[20] Thooyamani, K.P., Khanaa, V., & Udayakumar, R. (2013). Application of pattern recognition for farsi license plate recognition. *Middle-East Journal of Scientific Research*, *18*(12), 1768-1774.
[21] Jebaraj, S., Iniyan S. (2006). Renewable energy programmes in India. *International Journal of Global Energy Issues, 26*(43528), 232-257.
[22] Sharmila, S., & Jeyanthi Rebecca, L. (2013). Md Saduzzaman., Biodegradation of domestic effluent using different solvent extracts of Murraya koenigii. *J Chem and Pharm Res*, *5*(2), 279-282.
[23] Asiri, S., Sertkol, M., Guner, S., Gungunes, H., Batoo, K.M., Saleh, T.A., Manikandan A., & Baykal, A. (2018). Hydrothermal synthesis of CoyZnyMn1-2yFe2O4 nanoferrites: magneto-optical investigation. *Ceramics International*, *44*(5), 5751-5759.
[24] Rani, A.J., & Mythili, S.V. (2014). Study on total antioxidant status in relation to oxidative stress in type 2 diabetes mellitus. *Journal of clinical and diagnostic research: JCDR*, *8*(3), 108-110.
[25] Karthik, B. (2014). Arulselvi, Noise removal using mixtures of projected gaussian scale mixtures. *Middle-East Journal of Scientific Research*, *20*(12), 2335-2340.
[26] Karthik, B., Arulselvi, & Selvaraj, A. (2014). Test data compression architecture for low power VLSI testing. *Middle - East Journal of Scientific Research*, *20*(12), 2331-2334.
[27] Vijayaragavan, S.P., Karthik, B., & Kiran Kumar, T.V.U. (2014). Privacy conscious screening framework for frequently moving objects. *Middle-East Journal of Scientific Research*, *20*(8), 1000-1005.
[28] Kaliyamurthie, K.P., Parameswari, D., & Udayakumar, R. (2013). QOS aware privacy preserving location monitoring in wireless sensor network. *Indian Journal of Science and Technology*, *6*(5), 4648-4652.
[29] Silambarasu, A., Manikandan, A., & Balakrishnan, K. (2017). Room-temperature superparamagnetism and enhanced photocatalytic activity of magnetically reusable spinel ZnFe 2 O 4 nanocatalysts. *Journal of Superconductivity and Novel Magnetism, 30*(9), 2631-2640.
[30] Jasmin, M., Vigneshwaran, T., & Beulah Hemalatha, S. (2015). Design of power aware on chip embedded memory based FSM encoding in FPGA. *International Journal of Applied Engineering Research*, *10*(2), 4487-4496.
[31] Philomina, S., & Karthik, B. (2014). Wi-Fi energy meter implementation using embedded linux in ARM 9. *Middle-East Journal of Scientific Research*, *20*, 2434-2438.
[32] Vijayaragavan, S.P., Karthik, B., & Kiran Kumar, T.V.U. (2014). A DFIG based wind generation system with unbalanced stator and grid condition. *Middle-East Journal of Scientific Research, 20*(8), 913-917.
[33] Rajakumari, S.B., & Nalini, C. (2014). An efficient data mining dataset preparation using aggregation in relational database. *Indian Journal of Science and Technology, 7*, 44-46.
[34] Karthik, B., Kiran Kumar, T.V.U., Vijayaragavan, P., & Bharath Kumaran, E. (2013). Design of a digital PLL using 0.35 Î¼m CMOS technology. *Middle-East Journal of Scientific Research*, *18*(12), 1803-1806.
[35] Sudhakara, P., Jagadeesh, D., Wang, Y., Prasad, C.V., Devi, A.K., Balakrishnan, G., Kim B.S., & Song, J.I. (2013). Fabrication of Borassus fruit lignocellulose fiber/PP composites and comparison with jute, sisal and coir fibers. *Carbohydrate polymers*, *98*(1), 1002-1010.
[36] Kanniga, E., & Sundararajan, M. (2011). Modelling and characterization of DCO using pass transistors. In *Future Intelligent Information Systems,* 86(1), 451-457. Springer, Berlin, Heidelberg.
[37] Sachithanandam, P., Meikandaan, T.P., & Srividya, T. Steel framed multi storey residential building analysis and design. *International Journal of Applied Engineering Research*, *9*(22), 5527-5529.
[38] Kaliyamurthie, K.P., Udayakumar, R., Parameswari, D., & Mugunthan, S.N. (2013). Highly secured online voting system over network. *Indian Journal of Science and Technology*, *6*(S6), 4831-4836.
[39] Sathyaseelan, B., Manikandan, E., Lakshmanan, V., Baskaran, I., Sivakumar, K., Ladchumananandasivam, R., Kennedy, J., & Maaza, M. (2016). Structural, optical and morphological properties of post-growth calcined TiO2 nanopowder for opto-electronic device application: Ex-situ studies. *Journal of Alloys and Compounds*, *671*, 486-492.
[40] Saravanan, T., Sundar Raj M., & Gopalakrishnan K. (2014). SMES technology, SMES and facts system, applications, advantages and technical limitations. *Middle - East Journal of Scientific Research, 20*(11), 1353-1358.
[41] Sindhu, N., & Archana, M. (2015). An Investigation of a Double-Tail Comparator for Low-Power Applications. *International Scientific Journal on Science Engineering & Technology*, *18*(2), 48-63.
[42] Nair, P.G., & Loveleen, K.V. (2015). A Transformer less Single-Stage Single Switch AC/DC Converter with High Power Factor, Regulated Bus and Output Voltages. *International Scientific Journal on Science Engineering & Technology, 18*(4), 85-99.

[43] Ali, S.M., & Dr. Karule, P.T. (2015). Development of Automation System for Disease Disorder Diagnosis using Artificial Neural Networks and Support Vector Machine. *International Scientific Journal on Science Engineering & Technology, 18*(5), 103-112.
[44] Prichani, J.S., Sakwa, T.W., & Ongati, N.O., (2017). Smart Device based on GSM and GPS Technologies for Muliebrity Shielding. *The SIJ Transactions on Computer Science Engineering & its Applications, 5*(1), 13-15.
[45] Mallika, N.M., & Srinivasan, B. (2017). A Multi-Point Cluster for Maximization of Power Constraints in a Downlink Coordinated System. *The SIJ Transactions on Computer Science Engineering & its Applications, 5*(1), 16-19.
[46] Kumaravel, S., Nisha, G., Malathi, S., Malathy, R., & Madhubalasree, K. (2017). Connected Cars – The Future CarsDriven by Data. *The SIJ Transactions on Computer Science Engineering & its Applications, 5*(2), 1-3.
[47] Jayasarathi, M., Rajeshwari, S., Shiny Mercy, I., & Rathika, S.K.B. (2019). Enhanced on Data Encryption Standard for Secured Cloud Storage. *Bonfring International Journal of Software Engineering and Soft Computing, 9*(1), 7-10.
[48] Kavya, M.S., Dr.Geetha, B.G., & GokulRaaja, J.M. (2019). Android Application Development for Textile Industry. *Bonfring International Journal of Software Engineering and Soft Computing, 9*(1), 11-14.
[49] Vijayalakshmi, K. Bharathi, P., Deepika, N., Dennis Mary, S., & Jayathurga, B.(2017).Geographic based Hybrid Algorithm for Wireless Sensor Network. *The SIJ Transactions on Computer Networks & Communication Engineering (CNCE), 5*(2), 1-4.
[50] Kumaravel, S., Mohamed Thufail, H., Manoj Kumar, R., Karunyamani, V., & Mukesh Kumar, M.K. (2017). Energy Harvesting and Management from Ambient RF Radiation. *The SIJ Transactions on Computer Networks & Communication Engineering (CNCE), 5*(2), 5-9.